

## COMMUNICATION

Cite this: *J. Mater. Chem. A*, 2019, 7, 24784Received 8th August 2019  
Accepted 10th October 2019

DOI: 10.1039/c9ta08685d

rsc.li/materials-a

Non-corrosive, low-toxicity gel-based  
microbattery from organic and organometallic  
molecules†Frank N. Crespilho,<sup>a</sup> Graziela C. Sedenho,<sup>a,b</sup> Diana De Porcellinis,<sup>b</sup>  
Emily Kerr,<sup>c</sup> Sergio Granados-Focil,<sup>d</sup> Roy G. Gordon<sup>c</sup> and Michael J. Aziz<sup>a,b</sup>

Microbatteries with safe, non-corrosive electrolyte chemistries can have an immediate positive impact on modern life applications, such as ingestible electronic pills and system-on-chip bioelectronics. Here a safe, non-corrosive and non-flammable microbattery is reported. A natural agarose hydrogel is the electrolyte-supporting matrix, and organic and organometallic molecules are the redox-active species. This device can safely meet the needs of ingestible medical micro-devices as a primary battery. Additionally, this redox gel system can be used as a secondary battery for on-chip electronics applications, potentially enabling safe and cost-effective small-scale energy storage.

The current and future generations of micro- and nano-electronics include applications requiring a safe microbattery technology not available today. There is an increasing demand for microbatteries for applications such as environmental sensors, ingestible sensors (e-medical),<sup>1–3</sup> wireless communication devices,<sup>4</sup> autonomous microelectromechanical systems,<sup>5</sup> the internet of things,<sup>6,7</sup> sensor fusion,<sup>8,9</sup> wearable devices<sup>7,9,10</sup> and quantum computers.<sup>11</sup> Nanomaterials-based systems-on-a-chip have been specifically designed to be directly attached to a battery featuring ultra-low-power output, *e.g.* operation at near-threshold voltages of 0.6 V with a few microamperes of current.<sup>6</sup> Due to the challenges of miniaturizing energy storage technologies, microchips typically use power supplied off-chip,

limiting their autonomy, or use microbatteries with corrosive electrolytes, restricting their range of application.<sup>1–4,12</sup> Despite the fast-paced advances in microelectronics miniaturization<sup>3,6</sup> and integration,<sup>6</sup> there has been relatively slow progress in the miniaturization of power sources.

Here we report the development of a microbattery based on redox-gel active components that are non-corrosive, low-toxicity and non-flammable in contact with air or water. The gel is composed entirely of Earth-abundant elements and is safe to use in medical devices. We report the ability of organic redox active molecules to be incorporated into the hydrogel to form a redox-active gel (Fig. 1a) that acts as a stable, non-corrosive electrolyte at pH 7.0 in the body environment. This system can help to resolve corrosion and safety concerns of micro-battery chemistries currently available in the market, such as lithium ion<sup>1,3</sup> and silver-oxide.<sup>3</sup>

As illustrated in Fig. 1b the gel-based microbattery is composed of four parts: hydrogel-based negative side (gel-N), hydrogel-based positive side (gel-P), two flexible carbon fiber (FCF) microelectrodes, and a separator. Both gel-N and gel-P are composed of agarose, KCl, water, and a redox molecule. Bis(3-trimethylammonio) propyl viologen tetrachloride (BTMAP-Vi) and bis((3-trimethylammonio)propyl)ferrocene (BTMAP-Fc) were used in the gel-N and gel-P, respectively.<sup>13</sup> The redox active molecules were synthesized and purified as reported by Beh *et al.*<sup>13</sup> These molecules are well suited for gel batteries because both BTMAP-Fc and BTMAP-Vi show reversible and stable cyclic voltammetry behavior on FCF electrodes in 1.0 M KCl at pH 7.0 (Fig. 1c). Based on voltammetry, the theoretical cell voltage using these two molecules is expected to be approximately 0.75 V (Fig. 1c). The hydrogels are attractive due their structure and morphology, allowing diffusion of the redox active species, while maintaining predetermined shapes, as shown in Fig. 1b.

Agarose was chosen as the inert electrolyte support because it is widely available, low cost, mechanically versatile, safe for human consumption, stable at body temperature and prepared from naturally sourced polymers. One dollar's worth of agarose can be used to produce 770 batteries with 100  $\mu$ L of gel filling

<sup>a</sup>São Carlos Institute of Chemistry, University of São Paulo (USP), Av. Trabalhador São-carlense, 400, São Carlos, São Paulo 13560-970, Brazil. E-mail: frankcrespilho@usp.br

<sup>b</sup>Harvard School of Engineering and Applied Sciences, 29 Oxford Street, Cambridge, Massachusetts 02138, USA. E-mail: maziz@harvard.edu

<sup>c</sup>Department of Chemistry and Chemical Biology, Harvard University, 12 Oxford Street, Cambridge, Massachusetts 02138, USA

<sup>d</sup>Gustaf Carlson School of Chemistry and Biochemistry, Clark University, Worcester, Massachusetts 01610-1477, USA

† Electronic supplementary information (ESI) available: Synthesis of BTMAP-Vi and BTMAP-Fc, cyclic voltammetry, hydrogel preparation and cost, microbattery assembly and measurements, and capability of the microbattery to hold its charge. See DOI: 10.1039/c9ta08685d

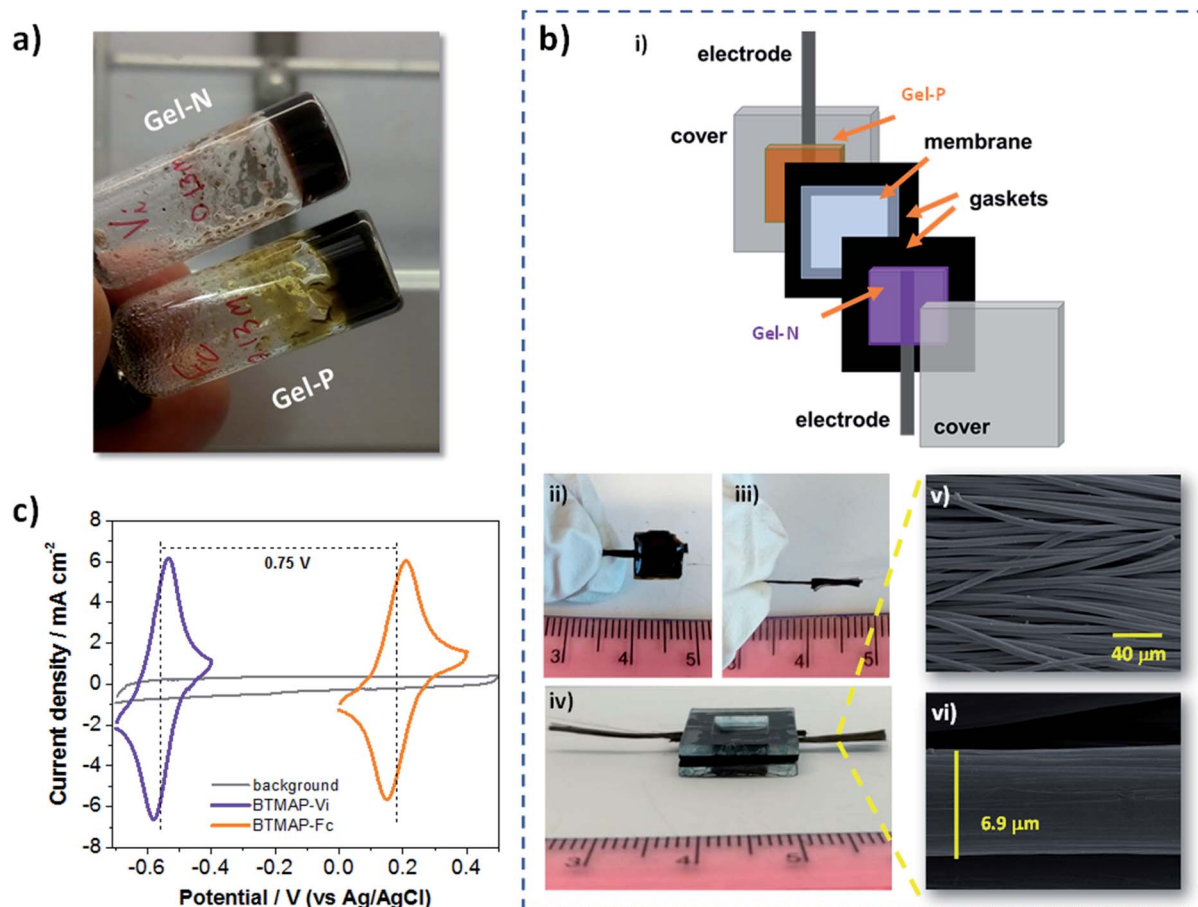


Fig. 1 (a) Gels containing agarose, KCl, and BTMAP-Vi (gel-N) and BTMAP-Fc (gel-P). (b) Scheme of the microbattery (i), photos of the gel on FCF electrode (ii and iii) and of the device (iv), and scanning electron microscopic images of FCF at different magnifications (v and vi). (c) Cyclic voltammograms of BTMAP-Vi and BTMAP-Fc and background recorded on FCF microelectrodes. Conditions: 2.0 mM of BTMAP-Vi and BTMAP-Fc in 1.0 M KCl, 50  $\text{mV s}^{-1}$ , Ar atmosphere. The expected cell potential is indicated.

each electrode compartment (see the calculation in the ESI<sup>†</sup>). The redox-gel was prepared using redox-active compounds (BTMAP-Fc or BTMAP-Vi) dissolved in an agarose gel. BTMAP-Fc and BTMAP-Vi exhibit relatively high diffusion coefficients in the hydrogel electrolyte,  $2.4 \times 10^{-6} \text{ cm}^2 \text{ s}^{-1}$  for BTMAP-Fc and  $2.8 \times 10^{-6} \text{ cm}^2 \text{ s}^{-1}$ , for BTMAP-Vi, as measured by PFGE-<sup>1</sup>H-NMR (see ESI<sup>†</sup>). These values are 20–27% lower than those for the same molecules measured at the same concentration in a KCl solution, ( $3.29 \times 10^{-6} \text{ cm}^2 \text{ s}^{-1}$  for BTMAP-Fc and  $3.45 \times 10^{-6} \text{ cm}^2 \text{ s}^{-1}$  for BTMAP-Vi).<sup>13</sup> Our measurements are consistent with a previous report.<sup>14</sup> Using the gel composition described in the ESI<sup>†</sup>, the redox-active molecules can readily diffuse through the hydrogel pores. In order to prevent redox-active molecule crossover, we inserted an anion-conducting membrane as a separator between the electrolyte gels, producing the cell shown in Fig. 1b. The concentration of redox molecules in each gel was 0.50 M and a Selemion DSV anion exchange membrane was used as the separator.

Fig. 2 shows the performance of these microbatteries. First, the cell was charged at 1.10 V for 30 min (to reach approximately 20% state of charge, SOC), and then a discharge curve was recorded at a constant current density of 20  $\mu\text{A cm}^{-2}$  (Fig. 2a).

This curve indicates that the microbattery can be discharged steadily over 100 h and provides a volumetric capacity of 0.021  $\mu\text{A h cm}^{-2} \mu\text{m}^{-1}$ . The microbattery can hold its charge for at least 48 h when no current is drained (Fig. S3 of the ESI<sup>†</sup>). The power curve in terms of current and power densities are shown in Fig. 2b. From this curve, we obtained an OCV of approximately 0.70 V and a maximum volumetric power density of 3.4  $\mu\text{W cm}^{-2} \mu\text{m}^{-1}$  at 8.7  $\mu\text{A cm}^{-2} \mu\text{m}^{-1}$  (20% SOC).

In order to evaluate the volumetric capacity, the microbattery was charged and discharged at a constant voltage of 1.10 V (to 92% SOC) and 0.30 V, respectively, as illustrated in Fig. 2c. The experimental volumetric capacity was calculated to be 1.42  $\text{mC cm}^{-2} \mu\text{m}^{-1}$ , which corresponds to 0.39  $\mu\text{A h cm}^{-2} \mu\text{m}^{-1}$  (or 3.94  $\mu\text{A h} \mu\text{L}^{-1}$ ), giving a total capacity of 0.79 mA h. This total capacity is lower than those measured for commercial lithium and silver-oxide microbatteries, 5 mA h and 80 mA h, respectively.<sup>3</sup> Nevertheless, these redox-gel microbatteries can power an ingestible sensor, requiring 4.69  $\mu\text{A}$ ,<sup>1</sup> for 168 h, and also other medical microdevices, as shown in Table 1.

Cycling tests were performed to evaluate the potential use of these redox-gel microbatteries as secondary batteries, (Fig. 2d and e). The coulombic efficiency for the galvanostatic cycling at

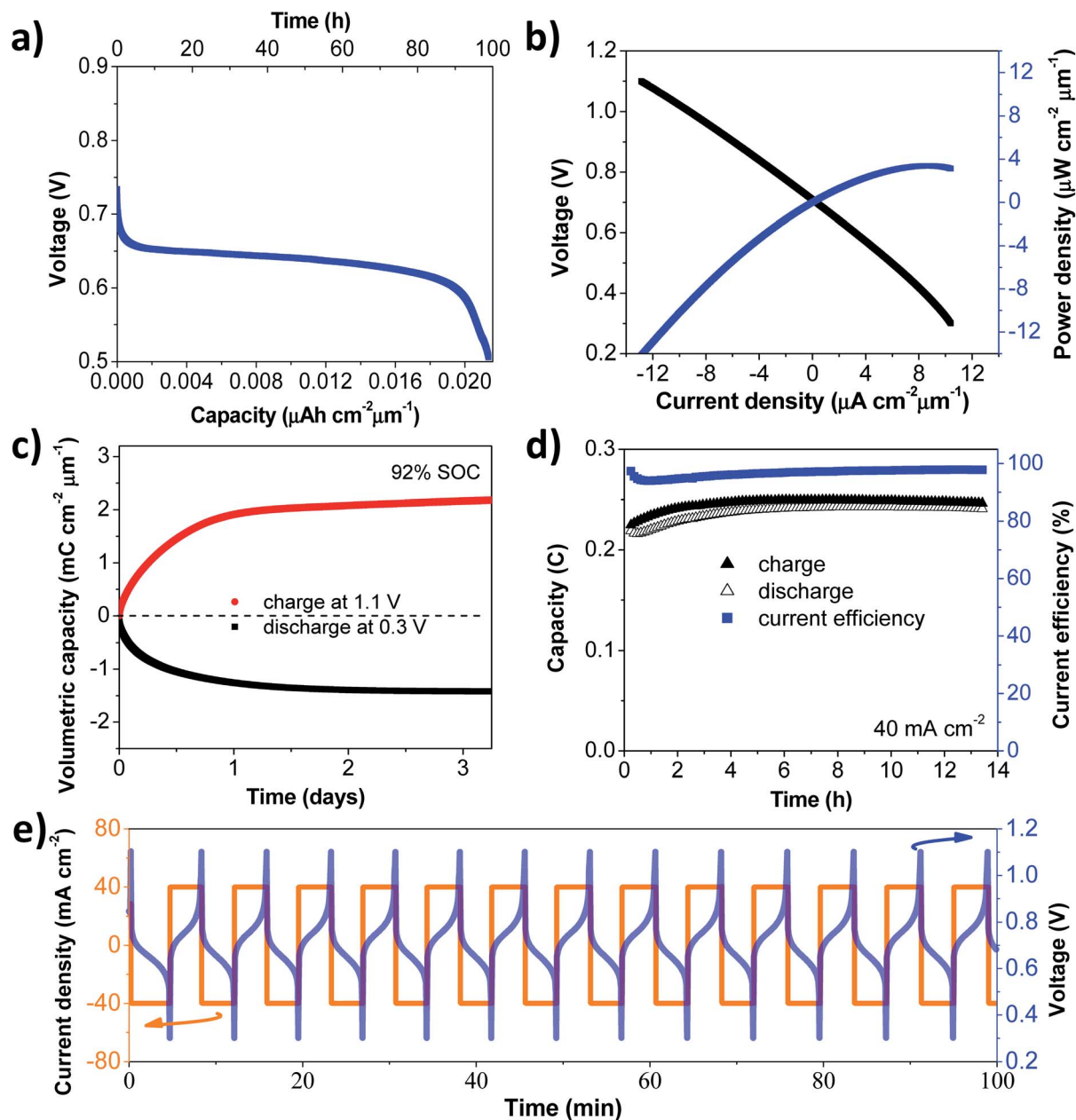


Fig. 2 (a) Voltage vs. time for galvanostatic discharge at  $40 \mu\text{A cm}^{-2}$ . (b) Cell voltage and power density vs. current density at 20% SOC. (c) Charge and discharge curves at 1.10 V and 0.30 V, respectively. (d) Capacity and current efficiency values of 100 cycles. (e) Representative voltage and current density vs. time curves during 100 charging–discharging cycles at  $40 \text{ mA cm}^{-2}$ . All data here were collected at room temperature, under  $\text{N}_2$  atmosphere, and using gel containing 1.0 M KCl and 0.50 M BTMAP-Fc on the positive side and gel containing 1.0 M KCl and 0.50 M BTMAP-Vi on the negative side, and Selemion DSV as anion exchange membrane.

$40 \text{ mA cm}^{-2}$  ranges between 94% and 97% during 13 h, corresponding to 100 cycles. The cycles are highly reproducible and indicate good electrochemical stability and a highly efficient storage system.

The size and non-corrosive composition of these redox-gel microbatteries constitute attractive advantages compared to typical lithium manganese button-cell and alkaline silver-oxide disk batteries.<sup>1</sup> The cells described in this work can be encased in volumes suitable to replace the traditional power sources within ingestible wireless endoscopy capsules,<sup>15</sup> or probiotic biosensors to monitor gastrointestinal health.<sup>1</sup> In contrast with

the low toxicity and non-corrosive nature of the microbatteries described here, accidental leakage of the electrolyte solution within alkaline silver-oxide disk batteries, can result in damage and in perforation of the esophagus if not removed surgically.<sup>16</sup> Similarly, a lithium microbattery<sup>1</sup> has a risk of burning in air or releasing a strongly corrosive solution and flammable hydrogen when in contact with water causing severe injuries.<sup>17</sup> The amounts of redox active molecules used in our redox-gel microbatteries are too small to produce harmful effects on humans. In terms of toxicity, viologens similar to those used in our battery have an oral LD 50 (lethal dose) of  $126 \text{ mg kg}^{-1}$  for

Table 1 Examples of low-power medical microdevices

System	Operation current ( $\mu\text{A}^a$ or $\mu\text{A MHz}^{-1b}$ )	Operation voltage (V)	Power consumption (nW)	Ref.
Ingestible biosensor to monitor gastrointestinal health	4.69 <sup>a</sup>	n/a	n/a	1
Integrated system-on-chip for internet of things, sensor fusion, wearables, and e-medical applications	9 <sup>b</sup>	0.5–0.6	n/a	6
Integrated circuit for miniature sensor nodes	n/a	0.6	3	20
Temperature sensor for low power wireless sensor nodes	n/a	0.075	71	21
Sensing, controlling and signal processing circuit for implantable CMOS	n/a	n/a	921	22

<sup>a</sup> Operation current in  $\mu\text{A}$ . <sup>b</sup> Operation current in  $\mu\text{A MHz}^{-1}$ .

rats, 22 mg kg<sup>-1</sup> for pigs, and 50 mg kg<sup>-1</sup> for monkeys. The lethal dose in humans is estimated to be about 7000 mg.<sup>18</sup> Our redox-gel microbatteries use a total of 29 mg of viologen derivative, which is 240 times smaller. Ferrocene derivatives show LD 50 of 25 mg kg<sup>-1</sup> for rats and 50 mg kg<sup>-1</sup> for mice.<sup>19</sup> Considering our microbattery contains 23 mg of ferrocene derivative, no harmful effect is expected for humans. In the event of accidental rupture while in the digestive system, this viologen/ferrocene-based microbattery poses a lower risk than the commercially available alternatives.

In summary, we describe a gel-based microbattery for use as a safe primary power source for several ingestible and implantable medical microdevices (Table 1). This gel-based approach can be expanded to include other redox molecules (e.g. natural product-based redox molecules) and can be further miniaturized. The combination of hydrogel and redox-active organic and organometallic molecules could represent an attractive strategy for developing non-toxic rechargeable microbatteries.

## Conflicts of interest

There are no conflicts to declare.

## Acknowledgements

This work was funded by the CNPq Brazil, FAPESP Brazil and U. S. NSF grant CBET-1509041. G. C. S. and F. N. C. gratefully acknowledge the financial support provided by the FAPESP (project numbers: 2015/22973-6, 2017/15714-0 and 2013/14262-7) and CNPq (project number: 203299/2017-5).

## References

- M. Mimeo, P. Nadeau, A. Hayward, S. Carim, S. Flanagan, L. Jerger, J. Collins, S. McDonnell, R. Swartwout, R. J. Citorik, V. Bulović, R. Langer, G. Traverso, A. P. Chandrakasan and T. K. Lu, *Science*, 2018, **918**, 915.
- A. T. Kutbee, R. R. Bahabry, K. O. Alamoudi, M. T. Ghoneim, M. D. Cordero, A. S. Almuslem, A. Gumus, E. M. Diallo, J. M. Nassar, A. M. Hussain, N. M. Khashab and M. M. Hussain, *npj flexible electronics*, 2017, **1**, 7.
- K. Kalantar-zadeh, N. Ha, J. Z. Ou and K. J. Berean, *ACS Sens.*, 2017, **2**, 468.
- H. Chen, S. Cartmell, Q. Wang, T. Lozano, Z. D. Deng, H. Li, X. Chen, Y. Yuan, M. E. Gross, T. J. Carlson and J. Xiao, *Sci. Rep.*, 2014, **4**, 3790.
- R. M. Iost, F. N. Crespilho, K. Kern and K. Balasubramanian, *Nanotechnology*, 2016, **27**, 29LT01.
- Y. Pu, C. Shi, G. Samson, D. Park, K. Easton, R. Beraha, A. Newham, M. Lin, V. Rangan, K. Chatha, D. Butterfield and R. Attar, *IEEE J. Solid-State Circuits*, 2018, **53**, 936.
- M. Haghi, K. Thurow and R. Stoll, *Healthc. Inform. Res.*, 2017, **23**, 4.
- R. Gravina, P. Alinia, H. Ghasemzadeh and G. Fortino, *Inform. Fusion*, 2017, **35**, 1339.
- V. J. Kartsch, S. Benatti, P. D. Schiavone, D. Rossi and L. Benini, *Inform. Fusion*, 2018, **43**, 66.
- Z. Liu, H. Li, M. Zhu, Y. Huang, Z. Tang, Z. Pei, Z. Wang, Z. Shi, J. Liu, Y. Huang and C. Zhi, *Nano Energy*, 2018, **44**, 164.
- M. Mohseni, P. Read and H. Neven, *Nature*, 2017, **543**, 171.
- K. Liu, Y. Liu, D. Lin, A. Pei and Y. Cui, *Sci. Adv.*, 2018, **4**, eaas9820.
- E. S. Beh, D. D. Porcellinis, R. L. Gracia, K. T. Xia, R. G. Gordon and M. J. Aziz, *ACS Energy Lett.*, 2017, **2**, 639.
- J. R. Lead, K. Starchev and K. J. Wilkinson, *Environ. Sci. Technol.*, 2003, **37**, 482.
- G. Iddan, G. Meron, A. Glukhovskiy and P. Swain, *Nature*, 2000, **405**, 417.
- M. Lupa, J. Mague, J. L. Guarisco and R. Amedee, *Ochsner J.*, 2009, **9**, 54.
- K. R. Jatana, K. Rhoades, S. Milkovich and I. N. Jacobs, *Laryngoscope*, 2017, **127**, 1276.
- U.S. National Library of Medicine, *Toxicology Data Network: Paraquat*, <https://toxnet.nlm.nih.gov/cgi-bin/sis/search/a?dbs+hsdb:@term+@DOCNO+1668>, accessed, January, 2019.
- U.S. National Library of Medicine, *Toxicology Data Network: 1-Acetylferrocene*, <https://chem.nlm.nih.gov/chemidplus/rn/1271-55-2>, accessed, March, 2019.
- P. Harpe, H. Gao, R. V. Dommele, E. Cantatore and A. H. M. van Roermund, *IEEE J. Solid-State Circuits*, 2015, **51**, 240.
- S. Jeong, Z. Foo, Y. Lee, J. Y. Sim, D. Blaauw and D. Sylvester, *IEEE J. Solid-State Circuits*, 2014, **49**, 1682.
- M. Poustinchi and S. Musallam, *Middle East Conference on Biomedical Engineering*, 2014, pp. 131–134.

## Electronic Supplementary Information

### Non-corrosive, Low-Toxicity Gel-based Microbattery from Organic and Organometallic Molecules

*Frank N. Crespilho,<sup>\*a,b</sup> Graziela C. Sedenho,<sup>a, b</sup> Diana De Porcellinis,<sup>b</sup> Emily Kerr,<sup>c</sup> Sergio Granados-Focil,<sup>d</sup> Roy G. Gordon,<sup>c</sup> and Michael J. Aziz<sup>\*b</sup>*

- a. São Carlos Institute of Chemistry, University of São Paulo (USP), Av. Trabalhador São-carlense, 400, São Carlos, São Paulo 13560-970, Brazil.
- b. Harvard School of Engineering and Applied Sciences, 29 Oxford Street, Cambridge, Massachusetts 02138, USA.
- c. Department of Chemistry and Chemical Biology, Harvard University, 12 Oxford Street, Cambridge, Massachusetts 02138, USA.
- d. Cambridge, Massachusetts 02138, USA.
- e. Gustaf Carlson School of Chemistry and Biochemistry, Clark University, Worcester, MA 01610-1477, USA.

#### Corresponding Authors

\* E-mails: frankcrespilho@usp.br, maziz@harvard.edu

## Experimental Methods

**Synthesis of BTMAP-Vi:** BTMAP-Vi was synthesized as previously described by Beh *et al.*<sup>1</sup> The scheme of its synthesis is shown in Figure S1a. Initially, 9.91 g (62.9 mmol) of 1-bromo-3-chloropropane was stirred with 6.6 mL (210.0 mmol) of a 25% solution of trimethylamine in methanol. After stirring at room temperature for 15 hours, the reaction mixture was diluted with ~50 mL of methyl tert-butyl ether (MTBE) and the suspended solid collected by vacuum filtration. The solid was rinsed with MTBE and dried in vacuo to give trimethyl(3-chloropropyl)ammonium bromide (**1**). Yield: 4.38 g (85.7%) of a fine white powder. This material was used without purification in the following step.

Then, 3.98 g (18.4 mmol) of **1** and 1.41g (9.0 mmol) of 4,4'-dipyridyl were suspended in ~10 mL of anhydrous DMF and heated to reflux under argon. Upon heating, all solids dissolved, followed shortly after by the formation of a large amount of pale yellow precipitate. After heating for 1 hour, the reaction mixture had partially solidified and had turned greenish. The reaction was cooled to room temperature and solid was collected by vacuum filtration, and then finally dried in vacuo to give (3-trimethylammonio)propyl viologen dibromide dichloride. The product was recrystallized by the addition of DMF to an aqueous solution. (**2**). Yield: 1.71 g (32.1%) of a pale-yellow powder.

A solution of 11.48 g (19.48 mmol) of **2** in ~100 mL of deionized H<sub>2</sub>O was passed through ~0.5 kg of wet Amberlite IRA-900 resin (chloride form). The resin was washed with ~1 L of deionized H<sub>2</sub>O. The eluted solution was evaporated in vacuo to give pure (3-trimethylammonio)propyl viologen tetrachloride (BTMAP-Vi). Yield: 9.76 g (99.9%) of an off-white deliquescent solid. <sup>1</sup>H NMR spectrum of the final product BTMAP-Vi is shown in Figure S1b.

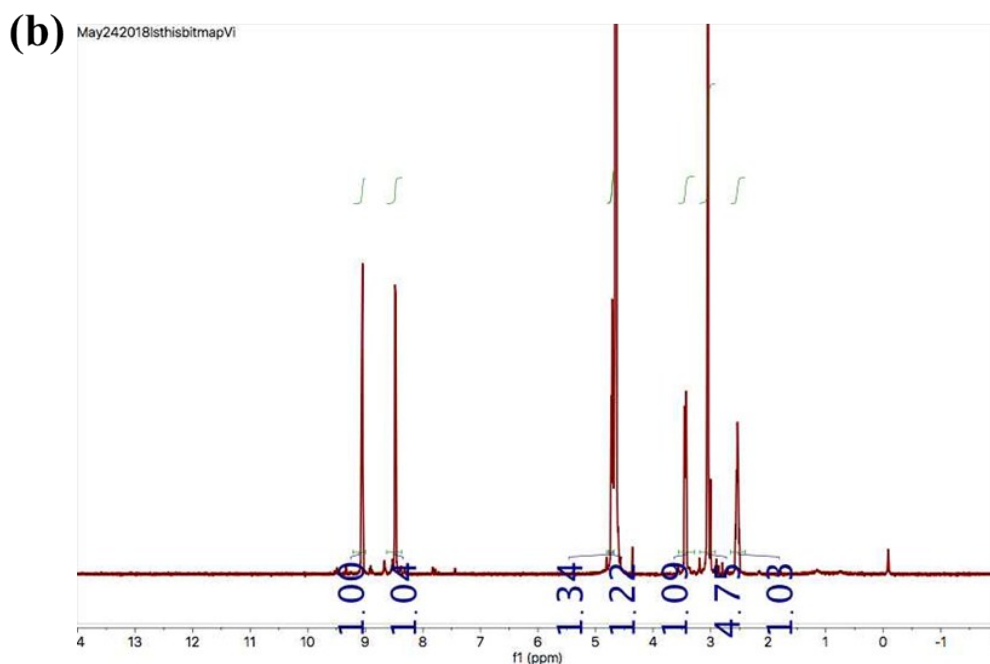
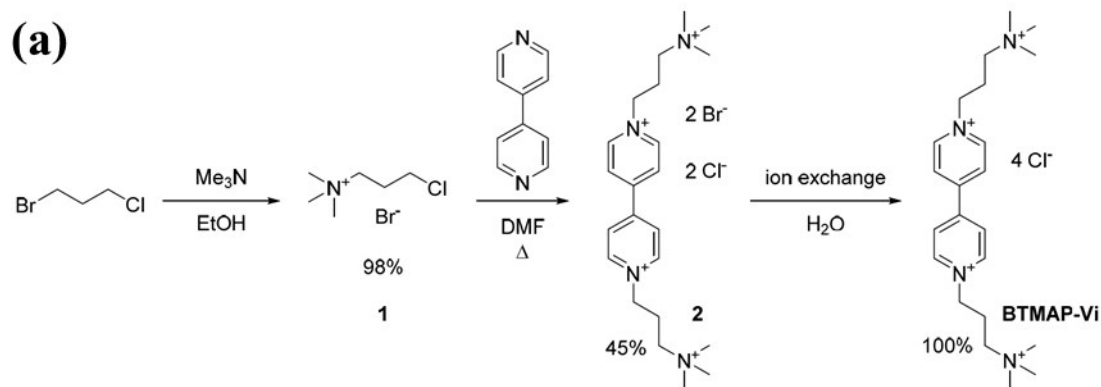
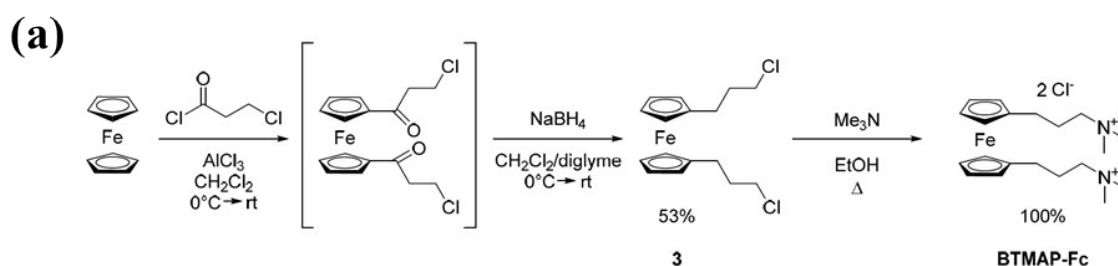


**Figure S1.** (a) Scheme of synthesis of BTMAP-Vi and (b) <sup>1</sup>H NMR spectrum of BTMAP-Vi recorded at 500 MHz, in D<sub>2</sub>O. δ 9.12 (d, 4H), 8.63 (d, 4H), 4.87 (t, 4H), 3.61 (m, 4H), 3.22 (s, 18H), 2.72 (m, 4H).

**Synthesis of BTMAP-Fc:** BTMAP-Fc was synthesized as previously described by Beh *et al.*<sup>1</sup> The scheme of its synthesis is shown in Figure S2a. Initially, 14.67 g (110.0 mmol) of AlCl<sub>3</sub> was suspended in ~100 mL of anhydrous CH<sub>2</sub>Cl<sub>2</sub>. A solution of 12.70 g (100.0 mmol) of 3-chloropropionyl chloride in ~50 mL of anhydrous CH<sub>2</sub>Cl<sub>2</sub> was added by syringe and the mixture stirred at room temperature for 2 hours. Once this was complete, the resulting slightly turbid golden-yellow solution was transferred *via* cannula into another flask, which had been

cooled to 0 °C, containing a solution of 9.30 g (50.0 mmol) of ferrocene in ~100 mL of anhydrous CH<sub>2</sub>Cl<sub>2</sub>. After stirring overnight, the reaction mixture was again cooled to 0 °C and a solution of 200 mL of 0.5 M NaBH<sub>4</sub> (100.0 mmol) in anhydrous diglyme was added *via* cannula and stirring was continued for a further 4 hours. Following that, the reaction was carefully quenched by the addition of ~500 mL of 1 M aqueous HCl. The organic phase was isolated and the aqueous phase extracted with CH<sub>2</sub>Cl<sub>2</sub> (3 × 100 mL). The extracts were combined, dried over anhydrous Na<sub>2</sub>SO<sub>4</sub>, filtered and evaporated to give the crude product of 1,1'-bis(3-chloropropyl)ferrocene (**3**). Yield: 16.02 g (94.5%) of a red-brown oil.

16.02 g (47.3 mmol) of column purified **3** was dissolved in ~100 mL of a 4.2 M solution of trimethylamine in ethanol. The solution was sealed in a heavy-walled glass tube and heated to 60 °C for 5 days. Following that, all volatiles were removed *in vacuo* to give a dark brown oil. The oil was stirred in H<sub>2</sub>O (~400 mL) and filtered to remove unreacted ferrocene and other water-insoluble impurities. The filtrate was evaporated *in vacuo* to give pure BTMAP-Fc. Yield: 20.76 g (96.1 %) of a dark brown glassy solid. <sup>1</sup>H NMR spectrum of the final product BTMAP-Fc is shown in Figure S2b.





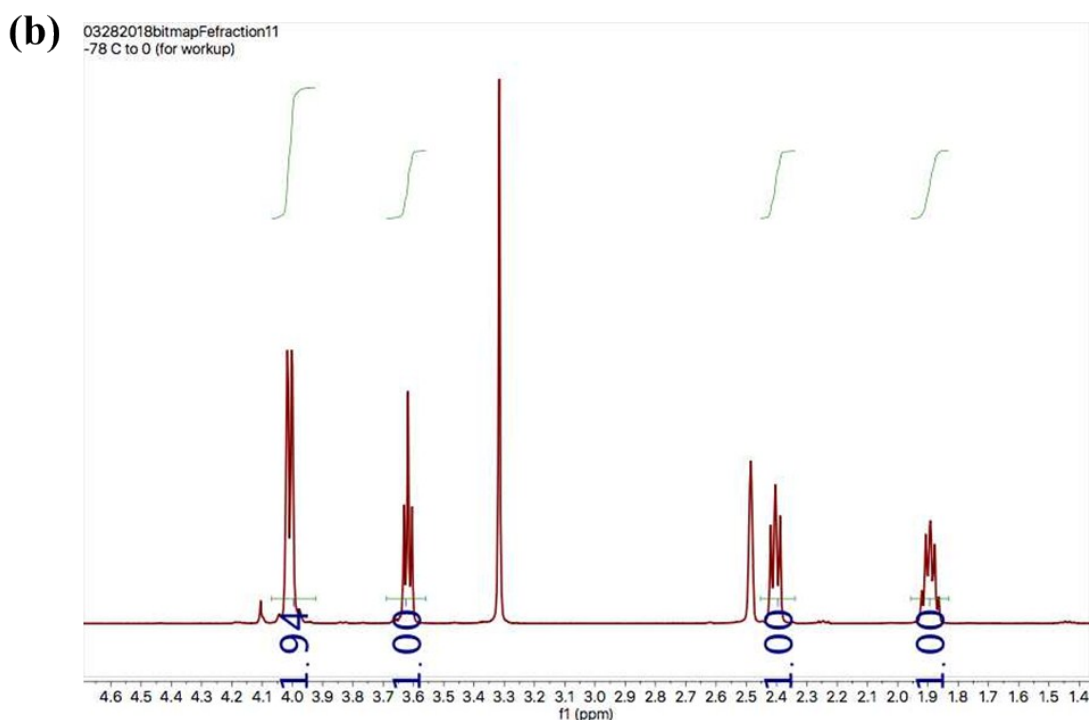


**Figure S2.** (a) Scheme of synthesis of BTMAP-Fc and  $^1\text{H}$  NMR spectrum of BTMAP-Fc recorded at 500 MHz, in  $\text{D}_2\text{O}$ .  $\delta$  4.15 (m, 8H), 3.27 (m, 4H), 3.05 (s, 18H), 2.55 (t, 4H), 1.94 (m, 4H).

**Cyclic voltammetry:** Cyclic voltammograms (CVs) were recorded in a Gamry Reference 3000 potentiostat (Gamry Instruments, United States) using an array of flexible carbon fibers (FCFs), Pt wire and Ag/AgCl electrode (3 M KCl filling solution) as working, counter and reference electrodes, respectively. Pt wire and Ag/AgCl electrode were obtained from BASi® (United States). Before the measurements, an array of FCFs was extracted from a carbon cloth (from Biolinker, Brazil) and chemically treated with  $\text{KMnO}_4$  in  $\text{H}_2\text{SO}_4$  solution.<sup>2</sup>

**Hydrogel preparation:** The hydrogels with BTMAP-Vi and BTMAP-Fc were prepared suspending 1.5 % (w/w) agarose in 1.0 M KCl containing 0.50 M of BTMAP-Vi and BTMAP-Fc. After, the suspensions were heated until 90 °C, because agarose dissolves in near-boiling water. Then, 100  $\mu\text{L}$  of each mixture was dropped on the top of FCF electrodes.

The system was cooled to room temperature to form the gels. The composition of the hydrogels is shown in table S1. At pH 7.0 both BTMAP-Fc and BTMAP-Vi are positively charged and highly soluble in water, almost up to 2.0 M for both reactants. However, BTMAP-Vi and BTMAP-Fc concentrations higher than 0.5 M were not used in the microbattery because they affect the agarose gelling. In addition, the agarose forms a water-swollen polymer network at room temperature, the crosslink density, and thus the diffusion of species absorbed within the hydrogel, can be controlled by tuning the agarose concentration.

**Table S1.** Composition of the BTMAP-Vi and BTMAP-Fc hydrogels.

<b>Component</b>	<b>% (w/w) in the</b>	<b>% (w/w) in the</b>
	<b>BTMAP-Fc hydrogel</b>	<b>BTMAP-Vi hydrogel</b>
<b>Agarose</b>	1.1 %	1.1 %
<b>KCl</b>	5.6 %	5.4 %
<b>BTMAP-Fc</b>	17.4 %	-
<b>BTMAP-Vi</b>	-	21.0 %
<b>Water</b>	75.8 %	72.5 %

**PFGE-<sup>1</sup>H-NMR measurements:** The diffusion coefficients of both BMAP-Vi and BTMAP-Fc were measured in 1M KCl solution in D<sub>2</sub>O and in a hydrogel with the same composition as table S1 using D<sub>2</sub>O instead of water. The measurements were made using a Varian INOVA, 600 MHz NMR spectrometer using a 5mm TRX/PFG triple resonance probe with a 70 gauss/cm maximum Z-gradient. Experiments were done using a 2 ms diffusion gradient length and a 150 ms diffusion delay time. The NMR data was processed using the built-in VNMR-J software from Varian.

**Microbattery assembly:** A microbattery with a Selemion DSV anion exchange separator was built with two polyacrylate pieces ( $1.50\text{ cm} \times 1.50\text{ cm} \times 1.50\text{ mm}$ ) with a pool ( $0.72\text{ cm} \times 0.72\text{ cm} \times 1.50\text{ mm}$ ) in the center to give a compartment for each gel. The dimensions of the entire microbattery are mainly attributed to the polyacrylate package. The separator was placed between the two compartments. The cell was gasketed by Viton sheets of  $270\text{ }\mu\text{m}$  in thickness.  $100\text{ }\mu\text{L}$  of heated mixture containing  $0.50\text{ M}$  BTMAP-Fc (positive side) and  $0.50\text{ M}$  BTMAP-Vi (positive side) in  $1.0\text{ M}$  KCl and  $1.5\%$  agarose were dropped in each compartment and cooled to room temperature to form the gel. One array of FCF was used as the electrode in each side of the battery, the geometric area exposed to the hydrogel was  $0.025\text{ cm}^2$ . The microbattery was sealed with silicone resin.

**Microbattery measurements:** Full cell tests were performed with a BioLogic BCS-815 battery cycling system. All measurements were carried out at room temperature and inside a glove bag in a  $\text{N}_2$  atmosphere. The charge and discharge current densities were calculated based on the anode area, which is  $0.025\text{ cm}^2$ . The measurements were carried out immediately after assembly of the microbattery. The microbattery was charged at  $1.10\text{ V}$  for  $30\text{ min}$ . If we define  $100\%$  SOC as the theoretical capacity ( $4.8\text{ C}$ ), then charging the battery at constant potential for  $30\text{ min}$ , achieves  $20\%$  SOC ( $0.89\text{ C}$ ). The polarization curve was obtained at  $\sim 20\%$  SOC by cyclic voltammetry where the potential is swept from  $0.30\text{ V}$  to  $1.10\text{ V}$  with a scan rate of  $100\text{ mV s}^{-1}$ . During the sweep in potential, the cell discharged less than  $0.05\text{ C}$ .

### Hydrogel cost

Agarose is a natural and low-cost polysaccharide used for preparation of hydrogels.<sup>3</sup> The price of laboratory grade agarose powder is around  $\$6.50$  per  $15\text{ g}$ . With  $15\text{ g}$  it is possible to

prepare 1.0 L of 1.5% agarose gel. Considering one microbattery is composed of 200  $\mu\text{L}$  of agarose gel (100  $\mu\text{L}$  of negolyte + 100  $\mu\text{L}$  of posolyte), with 1.0 L of gel it is possible to fabricate 5,000 microbatteries. This means that with \$1 it is possible to prepare hydrogel for 770 microbatteries at laboratory-scale prices.

### Capability of the microbattery to hold its charge

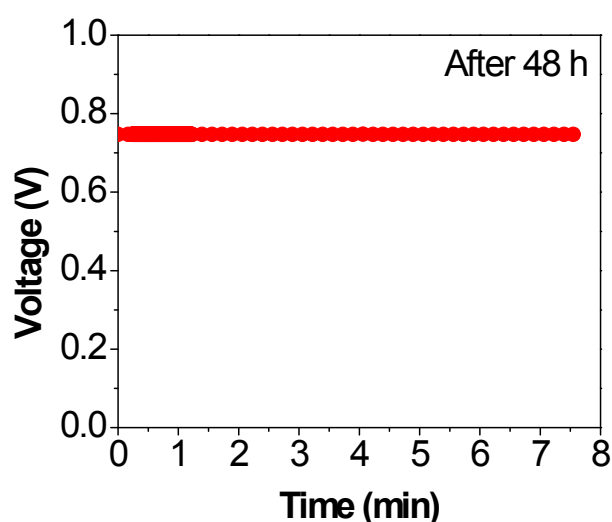


**Figure S3.** Measurement of cell voltage after 48 h of storage (no current drained).

### References

1. E. S. Beh, D. De Porcellinis, R. L. Gracia, K. T. Xia, R. G. Gordon, M. J. Aziz. *ACS Energy Lett.*, 2017, **2**, 639-644.
2. M. V. Martins, A. R. Pereira, R. S. Luz, R. M. Iost, F. N. Crespilho. *Phys. Chem. Chem. Phys.*, 2014, **16**, 17426-17436.
3. R. Armisen, F. Galata. Production, Properties and Uses of Agar. In *Production and utilization of products from commercial seaweeds*, Food and Agriculture Organization: Rome, Italy, 1987.